PHYSICAL REVIEW B VOLUME 51, NUMBER 5 1 FEBRUARY 1995-I

Elastic broadening of quasiparticle energy levels in vortex cores of high-T_c superconductors

R. Berkovits and B. Ya. Shapiro

The Jack and Pearl Resnick Institute for Advanced Technology, Department of Physics, Bar-Ilan University, Ramat-Gan 52900, Israel

(Received 16 June 1994; revised manuscript received 29 August 1994)

The influence of elastic scatterers, both short ranged as well as long ranged, on the density of quasiparticle energy states in the vortex cores of high-T_c superconductors is calculated. For short-range scatterers, the reduction of the density at energy values corresponding to the clean system's energy levels is exactly calculated by diagram summation. An expression for the broadening of the density of states (DOS) as a function of disorder is given. For long-range scatterers, the DOS as a function of the probability distribution of the scatterers is also calculated. In both cases a similar broadening of the DOS peaks is predicted. This might be useful in explaining experiments probing the density of states of vortex excitations.

While mesoscopic properties of low-dimensional, normal materials are now relatively well understood, electronic properties of mesoscopic superconductors and hybrid normal-metal–superconductor structures remain largely unexplored. Only recently have such hybrid structures begun to receive attention.[1–8] For the most part, experiment and theory have concentrated on electric properties of hybrid structures consisting of a superconductor with mesoscopic normal islands.[3–5] If the characteristic size of these islands does not exceed the superconducting coherence length ξ, varying in the range 10–1000 Å, superconductivity is induced inside the islands due to the proximity effect. This results in the appearance of a type of mesoscopic system consisting of a superconductor with a characteristic size much larger than the inelastic-scattering length and small regions in which superconducting excitations are confined due to Andreev reflection.[9] From this point of view, the cores of dirty Abrikosov vortices are one of the most easily realized mesoscopic systems of such a type.

In type II superconductors the magnetic field penetrates into the sample and forms a lattice of vortices. Such vortices are penetrated by one quantum flux Φ_0 each and are arranged in a triangular lattice. Near the vortices the superconducting gap function $\Delta(r)$ is reduced and there exist low-lying quasiparticle states which can be thermally excited.

The discrete excitation spectrum was predicted by Caroli, de Gennes, and Matricon.[10] In accordance with their theory, the energy scale of the quasiparticle spectrum in the vortex is set by the confinement energy $E_0 = h^2/m\xi^2$, where ξ is the superconducting coherence length. For high-temperature superconductors the coherence length is relatively short (of the order of $\xi \sim 10$ Å), and therefore the energy scale ($E_0 \sim 10$ meV) is large enough to be observed by far-infrared spectroscopy.

Recent experimental observation of the quasiparticle excitations in the vortex core confirms this theoretical picture,[11,12] although in both these experiments the energy levels are broadened. For conventional superconductors the quasiparticle levels are very close to each other and their discrete nature is lost,[12] while for high-T_c superconductors an explicit, rather large, broadening is measured.[11] This is expected since a set of clearly distinct excitation levels can exist only in extremely pure superconductors. In Ref. 11 the influence of nonelastic scattering of the core excitations was estimated using the well-known Abrikosov-Edwards theory.

The theoretical treatment of the influence of disorder on the density of states (DOS) of the vortex state was given by Kramer, Pesch, and Watts-Tobin[13,14] for conventional superconductors in which $\xi \gg l$ (where l is the electron mean free path). In that limit the discrete nature of the vortex states is completely lost. In this paper we shall calculate the contribution of elastic scattering off the impurities to the vortex quasiparticle level broadening for high-T_c superconductors in which $\xi \sim l$ and the vortex levels remain discrete. This is interesting since most high-T_c superconductors have a high concentration of impurities, and elastic scattering off those impurities might partially explain the large observed broadening of the vortex levels. Also, from the point of view of mesoscopic systems the vortex has the advantage of being a kind of naturally occurring mesoscopic system where the inelastic-scattering length is larger than its typical dimensions.

We shall start our treatment of the influence of elastic scattering on the low-lying quasiparticle vortex levels by considering the Bogoliubov–de Gennes (BdG) equation

$$\varepsilon\psi(\vec{r}) = \left[\frac{1}{2m}\left(\vec{p} - \sigma^z\frac{e}{c}\vec{A}\right)^2 + \gamma(\vec{r}) - E_F\right]\sigma^z\psi(\vec{r}) + \begin{pmatrix} 0 & \Delta(\vec{r}) \\ \Delta^*(\vec{r}) & 0 \end{pmatrix}\psi(\vec{r}), \quad (1)$$

where the gap function for a vortex centered at the origin and parallel to $\hat{z}$ is given in cylindrical coordinates (r,θ,z) by $\Delta(\vec{r}) = |\Delta(r)|\exp(-i\theta)$, $|\Delta(r)| \sim \Delta_0 r/\xi$ for

$r < \xi$ and $|\Delta(r)| \sim \Delta_0$ for $r > \xi$. σ^z is a Pauli matrix, while E_F is the Fermi energy. The short-range impurities are represented by $\gamma(\vec{r}) = \sum_i u_i \delta(\vec{r} - \vec{r}_i)$, where $\vec{r}_i$ are random locations of the impurities and u_i is their strength. This is an appropriate approximation for impurities of range smaller than the vortex dimensions. We shall discuss the situation for long-range impurities, i.e., scatterers of range much larger than the vortex dimension, later on.

For a clean vortex with no impurities ($u = 0$) Eq. (1) can be solved for weak magnetic fields $H \ll H_{c2}$.[10] The eigenfunctions of the low-lying excitations ($k_{F\|}\xi, \mu \ll k_{F\perp}\xi$) are, for $r < \xi$,

$$\psi^0_\mu(\vec{r}) \sim \left(\frac{k_{F\perp}}{2\pi\xi L_z}\right)^{1/2} e^{ik_{F\|}z} \times \begin{pmatrix} e^{i(\mu-\frac{1}{2})\theta} J_{\mu-\frac{1}{2}}(k_{F\perp}r) \\ e^{i(\mu+\frac{1}{2})\theta} J_{\mu+\frac{1}{2}}(k_{F\perp}r) \end{pmatrix}, \tag{2}$$

where the Fermi wave number $k_{F\perp} = k_F \cos\alpha$, $k_{F\|} = k_F \sin\alpha$, and α is an arbitrary angle. The angular quantum number $\mu = \pm 1/2, \pm 3/2, \ldots$. For $r > \xi$ the wave functions fall off exponentially. The eigenvalues for the clean case are[15]

$$\varepsilon^0_\mu = \frac{2\mu\Delta_0}{k_F v_F \cos^2\alpha}, \tag{3}$$

where a self-consistent logarithmic correction is neglected.[16]

The DOS for the low-lying vortex states can be calculated using the definition

$$\rho(\varepsilon) = -\frac{1}{\pi} \sum_{j=1}^{2} \Im \int d\vec{r}\; G^R_j(\vec{r}, \vec{r}, \varepsilon), \tag{4}$$

where the two components of the Green function are

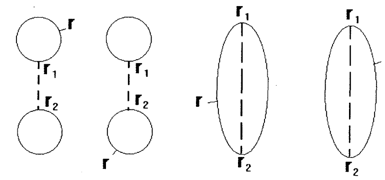

FIG. 1. The diagrammatic representation of the first order perturbative expansion of the averaged Green function given in Eq. (8). Full lines represent the free Green function $G^{0R}(\vec{r}, \vec{r}', \varepsilon)$, while the dashed line represents the averaged scattering potential $\langle \gamma(\vec{r})\sigma^z \gamma(\vec{r}')\sigma^z \rangle = u^2 I \delta(\vec{r} - \vec{r}')$.

$$G^R_j(\vec{r}, \vec{r}', \varepsilon) = \sum_\mu \frac{\psi^*_{\mu,j}(\vec{r})\psi_{\mu,j}(\vec{r}')}{\varepsilon - \varepsilon_\mu + i\Gamma}, \tag{5}$$

and Γ is an inelastic broadening which may be due to inelastic scattering into chain states or other inelastic processes. For a clean system one should replace ψ_μ with ψ^0_μ and ε_μ with ε^0_μ and thus obtain

$$\rho_0(\varepsilon) = \frac{1}{\pi} \sum_\mu \frac{\Gamma}{(\varepsilon - \varepsilon^0_\mu)^2 + \Gamma^2}, \tag{6}$$

which has the expected Lorentzian form.

The influence of disorder on the DOS will be taken into account by a perturbative expansion of the Green function with regard to the disorder strength. We assume the usual white noise statistics of the scatterers' positions and strengths, i.e.,

$$\langle \gamma(\vec{r})\sigma^z \rangle = 0,$$
$$\langle \gamma(\vec{r})\sigma^z \gamma(\vec{r}\,')\sigma^z \rangle = u^2 I \delta(\vec{r} - \vec{r}\,'), \tag{7}$$

where I is a 2×2 unit matrix, and $\langle \cdots \rangle$ denotes an ensemble averaging over different realizations of disorder. Therefore, the averaged Green function to lowest order in u^2 is given by

$$\begin{aligned}
\langle G^{1R}_j(\vec{r}, \vec{r}, \varepsilon) \rangle = u^2 &\int d\vec{r}_1\, d\vec{r}_2\; G^{0R}_j(\vec{r}, \vec{r}_1, \varepsilon)\; G^{0R}_j(\vec{r}_1, \vec{r}_2, \varepsilon)\; G^{0R}_j(\vec{r}_2, \vec{r}, \varepsilon)\; \delta(\vec{r}_1 - \vec{r}_2) \\
+u^2 &\int d\vec{r}_1\, d\vec{r}_2\; G^{0R}_j(\vec{r}_1, \vec{r}, \varepsilon)\; G^{0R}_j(\vec{r}, \vec{r}_2, \varepsilon)\; G^{0R}_j(\vec{r}_2, \vec{r}_1, \varepsilon)\; \delta(\vec{r}_1 - \vec{r}_2) \\
+u^2 &\int d\vec{r}_1\, d\vec{r}_2\; G^{0R}_j(\vec{r}, \vec{r}_1, \varepsilon)\; G^{0R}_j(\vec{r}_1, \vec{r}, \varepsilon)\; G^{0R}_j(\vec{r}_2, \vec{r}_2, \varepsilon)\; \delta(\vec{r}_1 - \vec{r}_2) \\
+u^2 &\int d\vec{r}_1\, d\vec{r}_2\; G^{0R}_j(\vec{r}_1, \vec{r}_1, \varepsilon)\; G^{0R}_j(\vec{r}, \vec{r}_2, \varepsilon)\; G^{0R}_j(\vec{r}_2, \vec{r}, \varepsilon)\; \delta(\vec{r}_1 - \vec{r}_2),
\end{aligned} \tag{8}$$

which is represented in a diagrammatic way in Fig. 1. Performing the integrations one obtains that the correction to the averaged DOS to first order in u^2 is

$$\delta\rho_1(\varepsilon) = -\frac{2u^2}{\pi V} \Im \sum_{\mu_1,\mu_2} \left(\frac{1}{(\varepsilon - \varepsilon^0_{\mu_1}) + i\Gamma}\right)^2 \times \left(\frac{1}{(\varepsilon - \varepsilon^0_{\mu_2}) + i\Gamma}\right), \tag{9}$$

where $V = \pi L_z \xi^2$ is the volume of the vortex. In Fig. 2 we plot $\delta\rho_1$ as a function of ε. It can be seen that the correction to the DOS has a form of an antipeak around values of energy corresponding to ε^0_μ. Therefore the total DOS to the first order in u^2 will have local minima at the positions of the clean system energy levels, which seems to be unphysical. The reason for this peculiar behavior is that it is not sufficient to sum the perturbative expansion to the first order in u^2. Thus, especially for values of energy close to ε^0_μ, higher-order corrections must be considered.

As can be seen in Eq. (9) for $\varepsilon = \varepsilon^0_\mu$ the main contribution (as long as the initial level broadening is smaller than the distance between consecutive energy lev-

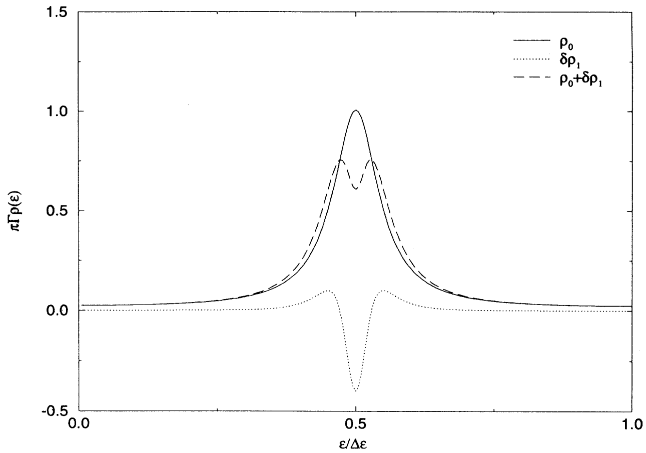

FIG. 2. The first order correction to the DOS $\delta\rho_1(\varepsilon)$ as function of the energy in the vicinity of $\varepsilon^0_{\mu=1}$, for $u/\sqrt{2V}\Gamma = 1/3$. The full line corresponds to the clean system DOS ρ_0, the dotted line to $\delta\rho_1$, and the dashed line to the first order DOS $\rho_0 + \delta\rho_1$.

els, i.e., $\Gamma < \Delta\varepsilon \equiv 2\Delta_0/k_F v_F \cos^2\alpha$) comes from the $\mu_1 = \mu_2 = \mu$ term in the summation. This is correct for all the diagrams at any order of u. Moreover, at this point all diagrams of the same order m in u (or in another language, the same number of impurity lines) have the same contribution

$$\frac{(-1)^m}{\pi}\left(\frac{u^2}{2V}\right)^m \Gamma^{-(2m+1)}. \tag{10}$$

Therefore at $\varepsilon = \varepsilon^0_\mu$ the calculation of the mth order correction to the DOS is reduced to counting the number of diagrams of the mth order. Examples of such diagrams are presented in Fig. 3. The number of diagrams of the mth order is

$$N_m = 2m \sum_{l_1 \geq l_2 \geq \cdots l_{2m}=1}^{2m} C(l_1, l_2, \ldots, l_{2m}) \times \frac{2m! f(l_1) f(l_2) \cdots f(l_{2m})}{l_1! l_2! \cdots l_{2m}!} \delta_{l_1+l_2+\cdots+l_{2m}, 2m}, \tag{11}$$

where $f(l) = (l-1)!/2$ for $l > 3$ and $f(l) = 1$ for $l \leq 3$, and $C(l_1, l_2, \ldots l_{2m}) = 1/(j_1! j_2! \ldots j_{2m}!)$ where j_i is the number of summation variables l equal to i. Thus the correction of the mth order to the DOS is

$$\delta\rho_m(\varepsilon = \varepsilon^0_\mu) = N_m \frac{(-1)^m}{\pi\Gamma}\left(\frac{u}{\sqrt{2V}\Gamma}\right)^{2m}, \tag{12}$$

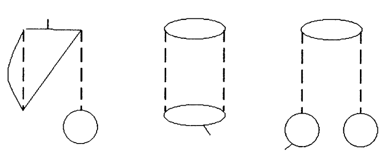

FIG. 3. Several diagrams contributing to the second order correction to the DOS.

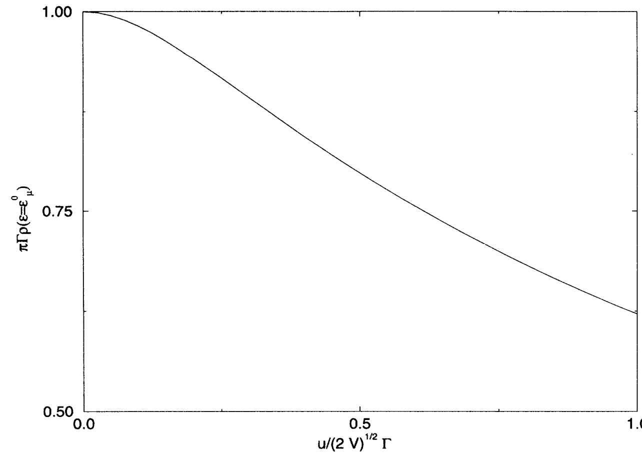

FIG. 4. The DOS at $\varepsilon = \varepsilon^0_\mu$ as a function of the disorder $\frac{u}{\sqrt{2V}\Gamma}$.

and the exact averaged DOS at the original energy level is

$$\rho(\varepsilon = \varepsilon^0_\mu) = \sum_{m=0}^{\infty} \delta\rho_m(\varepsilon = \varepsilon^0_\mu). \tag{13}$$

For large values of m the most important contribution to N_m comes from the highly connected diagrams which give a contribution of $2m!$ (up to logarithmic corrections). Therefore the summation can be written as

$$\rho(\varepsilon = \varepsilon^0_\mu) \sim \frac{1}{\pi\Gamma}\sum_{m=0}^{\infty}(-1)^m 2m! \left(\frac{u}{\sqrt{2V}\Gamma}\right)^{2m}. \tag{14}$$

This divergent series may be summed using Borel summation[17] resulting in

$$\rho(\varepsilon = \varepsilon^0_\mu) \sim \frac{1}{\pi\Gamma}\int_0^\infty \frac{e^{-t}dt}{1+\left(\frac{ut}{\sqrt{2V}\Gamma}\right)^2}, \tag{15}$$

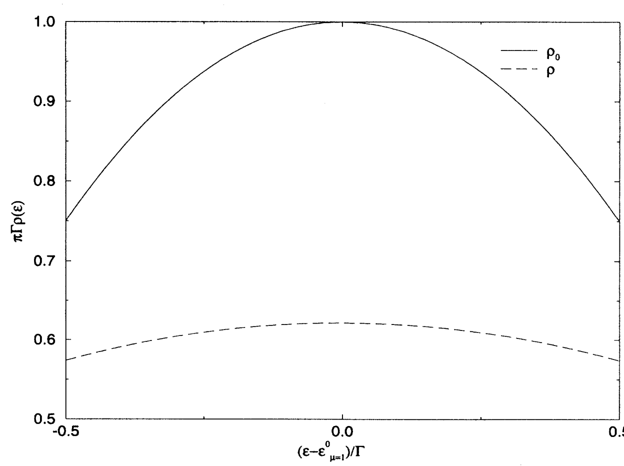

FIG. 5. The shape of the DOS in the regime of $\varepsilon = \varepsilon^0_\mu$. The full line represents the shape in the absence of scatterers and the dashed line represents it in the case of $\frac{u}{\sqrt{2V}\Gamma} = 1$.

plotted in Fig. 4. It may be seen that there is a monotonic reduction in the peak height as function of the disorder $u/\sqrt{2V}\Gamma$. Following the previous steps it is also possible to expand the DOS for values close to ε^0_μ, as long as $(\varepsilon - \varepsilon^0_\mu)/\Gamma < 1$. Then one obtains

$$\rho(\varepsilon) \sim \rho(\varepsilon = \varepsilon^0_\mu) - \frac{1}{\pi\Gamma}\left(\frac{\varepsilon - \varepsilon^0_\mu}{\Gamma}\right)^2 \times \sum_{m=0}^{\infty} (-1)^m 2m!(m+1)(2m+1)\left(\frac{u}{\sqrt{2V}\Gamma}\right)^{2m}, \tag{16}$$

which after summation results in

$$\rho(\varepsilon) \sim \rho(\varepsilon = \varepsilon^0_\mu) - \frac{1}{\pi\Gamma}\left(\frac{\varepsilon - \varepsilon^0_\mu}{\Gamma}\right)^2 \frac{1}{2}\int_0^\infty \frac{e^{-t}t^2 dt}{1 + \left(\frac{ut}{\sqrt{2V}\Gamma}\right)^2}, \tag{17}$$

which for a particular value of disorder strength is plotted in Fig. 5. It is interesting to note that as the degree of disorder becomes bigger the height of the peak is reduced while its width increases. This behavior should be expected since the number of states does not change due to the elastic scattering and therefore the total area of the peak should be conserved. In order to estimate the degree of broadening of the peak one can compare the coefficient of $[(\varepsilon - \varepsilon^0_\mu)/\Gamma]^2$ relative to $\rho(\varepsilon = \varepsilon^0_\mu)$ as a function of disorder, which for the clean case is equal to 1, while for the disordered case it is equal to

$$B(u/\sqrt{2V}\Gamma) = \frac{1}{2}\int_0^\infty \frac{e^{-t}t^2 dt}{1 + \left(\frac{ut}{\sqrt{2V}\Gamma}\right)^2} \Bigg/ \int_0^\infty \frac{e^{-t} dt}{1 + \left(\frac{ut}{\sqrt{2V}\Gamma}\right)^2}, \tag{18}$$

plotted in Fig. 6. It is clear that, as the disorder $u/\sqrt{2V}\Gamma$ increases, $B(u/\sqrt{2V}\Gamma) \sim \sqrt{2V}\Gamma/u$ decreases, corresponding to a relative broadening of the DOS as a function of disorder.

We have until now discussed the influence of scatterers which are of smaller dimensions than the vortex cores (short-range scatterers). In the opposite limit, where the scattering potential is smooth on the scale of the vortex core, the scattering potential $\gamma(\vec{r})$ in Eq. (1) can be replaced by γ_i which depends on the particular configuration of the scatterers in the vicinity of the vortex. Thus, according to Eq. (3) the energy levels for a particular vortex will be given by $\varepsilon_{\mu,i} = \hbar\mu\Delta_0/(E_F - \gamma_i)\cos^2\alpha$ which for $\gamma_i \ll E_F$ may be written as $\varepsilon_{\mu,i} = \varepsilon^0_\mu(1 + \gamma_i/E_F)$. Therefore, although the Fermi energy is constant across the sample, there are local shifts in the energy levels of particular vortices as a result of the renormalization of the local electron density. Assuming that the distribution of the local potentials $P(\gamma_i)$ is known, the averaged DOS is given by

$$\rho(\varepsilon) = \frac{\Gamma}{\pi}\sum_\mu \int d\gamma_i \frac{P(\gamma_i)}{[\varepsilon - \varepsilon^0_\mu(1 + \gamma_i/E_F)]^2 + \Gamma^2}, \tag{19}$$

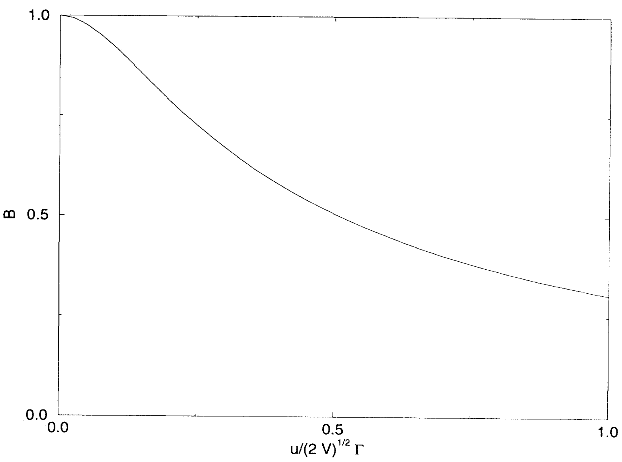

FIG. 6. The relative broadening $B(u/\sqrt{2V}\Gamma)$ of the peak as a function of disorder.

which will result in the broadening of the averaged DOS. As an example, for a flat distribution $P(\gamma_i) = 1/W$ in the range $-W/2 < \gamma_i < W/2$ one gets

$$\rho(\varepsilon) = \frac{1}{\pi W}\sum_\mu \tan^{-1}\left(\frac{\varepsilon - \varepsilon^0_\mu(1 + W/2E_F)}{\Gamma}\right) - \tan^{-1}\left(\frac{\varepsilon - \varepsilon^0_\mu(1 - W/2E_F)}{\Gamma}\right), \tag{20}$$

which is plotted in Fig. 7. The reduction in the peak height as well as the broadening of the peak are clearly seen.

In a realistic experimental situation the scatterers are expected to have a range intermediate between the point scatterer case described in the beginning of the paper and the very-long-ranged scatterer case just discussed. Since both cases give the same qualitative behavior, i.e., a

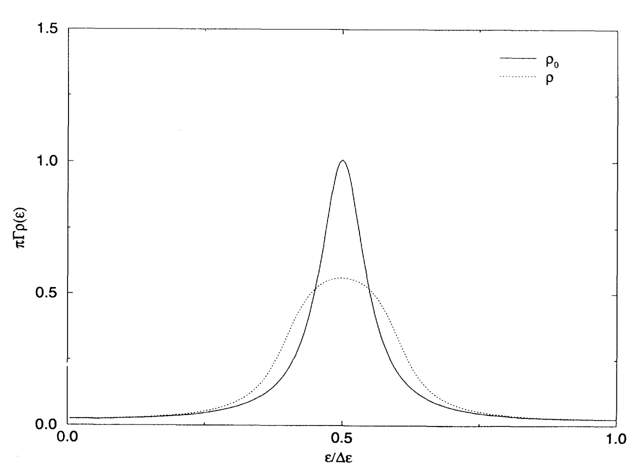

FIG. 7. The DOS in the vicinity of $\varepsilon^0_{\mu=1}$ for long-range scatterers. The full line corresponds to ρ_0 and the dotted line to the disordered case with $\varepsilon^0_{\mu=1}W/E_F = 4\Gamma$.

broadening of the DOS peak which increases as a function of disorder, one might expect that the presence of any kind of elastic scatterers in the superconductor will have a similar effect on the DOS. This effect can be measured by far-infrared spectroscopy techniques, akin to the ones used in Ref. 11. Thus, by changing the concentration of elastic scatterers, their explicit influence on the DOS can be studied.

In conclusion, the influence of elastic scatterers on the averaged DOS of quasiparticles in vortex cores has been explicitly calculated for point scatterers, using a perturbative expansion, as well as for long-range scatterers. In both cases a mesoscopic broadening of the DOS peaks is predicted due to the elastic scatterers. Therefore, in addition to the usual inelastic broadening traditionally considered in these systems, a second mechanism of elastic broadening exists which may explain the experimentally measured broadening.

We would like to thank Y. Avishai for useful discussions. R.B. would like to thank the Alon Foundation and the U.S.–Israel Binational Science Foundation for financial support. B.S. thanks the Guastella foundation and the Ministry of Science and Arts of Israel for support.

[1] B. Z. Spivak and D. E. Khmelnitskii, JETP Lett. **35**, 413 (1982).
[2] B. L. Altshuler and B. Z. Spivak, Sov. Phys. JETP **65**, 343 (1987).
[3] C. W. J. Beenakker and H. van Houten, Phys. Rev. Lett. **66**, 3056 (1991).
[4] L. I. Glazman and K. A. Matveev, JETP Lett. **49**, 659 (1989).
[5] C. W. J. Beenakker, Phys. Rev. Lett. **67**, 3863 (1991).
[6] V. C. Hui and C. J. Lambert, Europhys. Lett. **23**, 203 (1993).
[7] C. J. Lambert, J. Phys. Condens. Matter **5**, 707 (1993).
[8] C. J. Lambert, J. Phys. Condens. Matter **3**, 6759 (1991).
[9] A. F. Andreev, Sov. Phys. JETP **19**, 1228 (1964).
[10] C. Caroli, P. G. de Gennes, and J. Matricon, Phys. Lett. **9**, 307 (1964).
[11] K. Karrai, E. J. Choi, F. Dunmore, S. Liu, H. D. Drew, Q. Li, D. B. Fenner, Y. D. Zhu, and F. Zhang, Phys. Rev. Lett. **69**, 152 (1992).
[12] H. F. Hess, R. B. Robinson, R. C. Dynes, J. M. Valles, Jr., and J. V. Waszczak, Phys. Rev. Lett. **62**, 214 (1989); J. D. Shore *et al.*, *ibid.* **62**, 3089 (1989).
[13] L. Kramer, W. Pesch, and R. J. Watts-Tobin, Solid State Commun. **14**, 1251 (1974).
[14] L. Kramer, W. Pesch, and R. J. Watts-Tobin, J. Low Temp. Phys. **14**, 29 (1974).
[15] L. Kramer and W. Pesch, Z. Phys. **269**, 59 (1974).
[16] T. C. Hsu, Phys. Rev. B **46**, 3680 (1992).
[17] C. M. Bender and S. A. Orszag, *Advanced Mathematical Methods for Scientists and Engineers* (McGraw-Hill, New York, 1978).